SSCL-526

SSCL-526

Superconducting Super Collider Laboratory

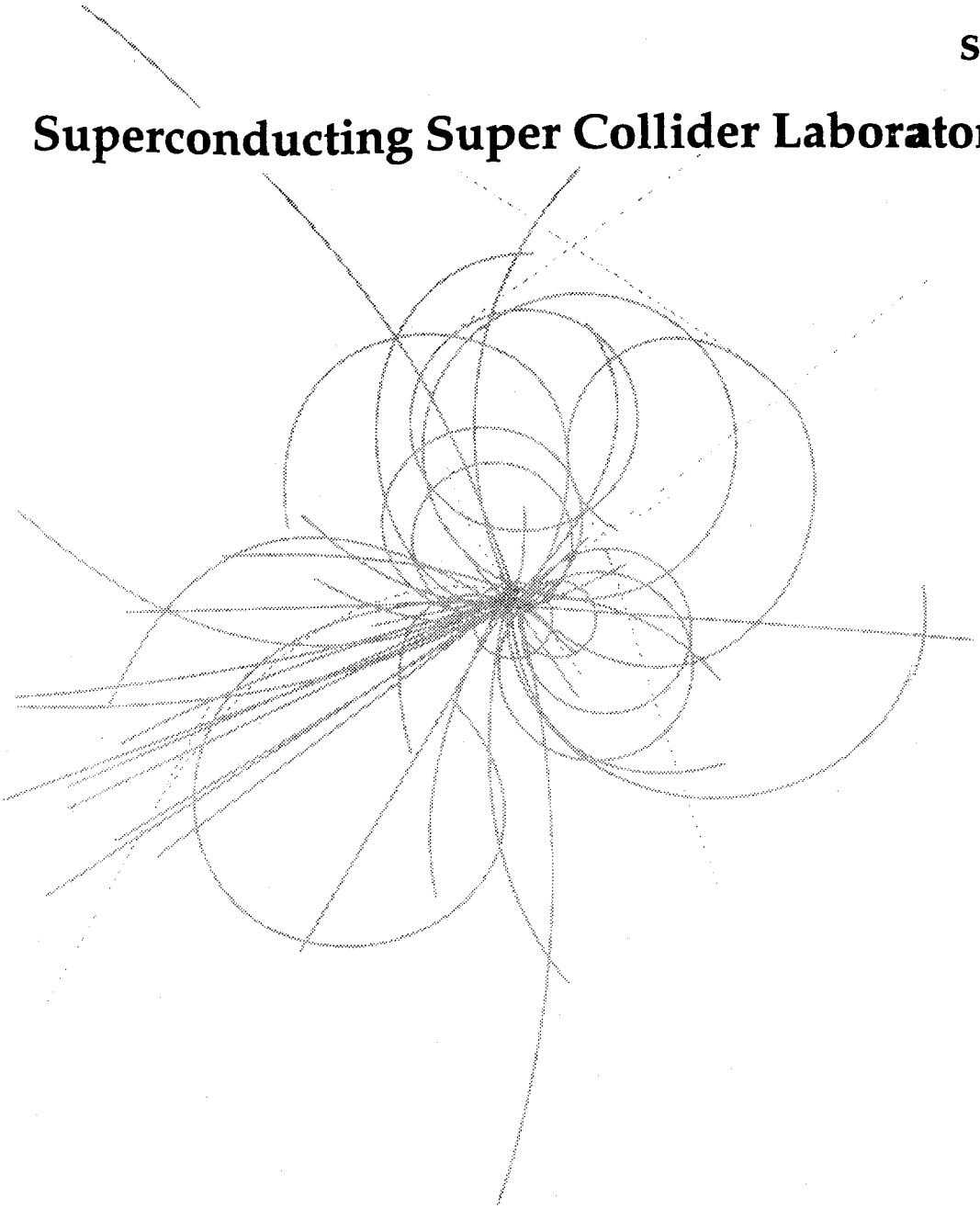

Analysis of ER String Test Thermally Instrumented Interconnect 80-K MLI Blanket

E. Daly and R. Pletzer

April 1992

SSCL-526

Analysis of ER String Test Thermally Instrumented Interconnect 80-K MLI Blanket

E. Daly and R. Pletzer

Magnet Systems Division
Superconducting Super Collider Laboratory*
2550 Beckleymeade Ave.
Dallas, TX 75237

April 1992

*Operated by the Universities Research Association, Inc., for the U.S. Department of Energy under Contract No. DE-AC35-89ER40486.

CONTENTS

FIGURES v
TABLES v
1.0 INTRODUCTION 1
2.0 ANALYSIS 1
2.1 Thermal Modeling 2
2.1.1 Thermal Radiation Component 3
2.1.2 Gas Conduction Component 4
2.1.3 Spacer Conduction Component 5
2.2 Analysis Cases 6
3.0 RESULTS 7
3.1 Heavy Cover Layer Effective Properties 7
3.2 Predicted Temperature Gradients 7
3.3 Predicted 80-K Blanket Assembly Heat Flux and Gradients 8
4.0 CONCLUSIONS AND RECOMMENDATIONS 9
REFERENCES 11

FIGURES

1. Thermally Instrumented 80-K MLI Blanket Assembly 2
2. MLI Thermal Model 3
3. Comparison of Measured and Predicted Temperatures vs. Blanket Layer Number on 10/1/91 8
4. Comparison of Measured and Predicted Temperatures vs. Blanket Layer Number on 10/23/91 8

TABLES

1. Predicted Heat Fluxes and Effective Resistances 9

1.0 INTRODUCTION

An 80-K Multi Layer Insulation (MLI) blanket in the interconnect region between magnets DD0019 and DD0027 in the Fermi National Accelerator Laboratory (FNAL) ER string was instrumented with temperature sensors to obtain the steady-state temperature gradient through the blanket after string cooldown. A thermal model of the 80-K blanket assembly was constructed to analyze the steady-state temperature gradient data. Estimates of the heat flux through the 80-K MLI blanket assembly and predicted temperature gradients were calculated.

The thermal behavior of the heavy polyethylene terapthalate (PET) cover layers separating the shield and inner blanket and inner and outer blankets was derived empirically from the data. The results of the analysis predict a heat flux of 0.363–0.453 W/m^2 based on the 11 sets of data. These flux values are 33–46% below the 80-K MLI blanket heat leak budget of 0.676 W/m^2. Predictions of the temperature gradients compared generally well with the measured data, but they tended to underpredict temperatures at each sensor location and to produce a flatter gradient than the measured data showed.

The effective thermal resistance of the two heavy PET cover layers between the shield and inner blanket was found to be 2.1 times that of a single PET spacer layer, and the effective resistance of the two heavy PET cover layers between the inner blanket and outer blanket was found to be 7 times that of a single PET spacer layer. These effective resistances for the heavy PET layers were found to adequately predict the temperature gradient through these layers for all data cases.

Based on these results, the 80-K MLI blanket assembly appears to be performing more than adequately to meet the 80-K static IR heat leak budget. However, these results should not be construed as a verification of the 80-K static IR heat leak, since no actual heat leak was measured. The results have been used to improve the empirically based model data in the 80-K MLI blanket thermal model, which has previously not included the effects of heavy PET cover layers on 80-K MLI blanket thermal performance.

2.0 ANALYSIS

The 80-K MLI blanket assembly instrumented for this analysis consists of two 32-layer MLI blankets wrapped once each around the 80-K shield bridge in the interconnect region between magnet nos. 19 and 27 in the ER string. Each MLI blanket consists of 32 layers of 0.25-mm-thick Double Aluminized Mylar (DAM) reflector material separated by single layers of 0.1-mm-thick PET spacer material. The blankets have DAM reflector layers on the outside. The 80-K shield and inner blanket and inner and outer blankets are separated by two layers of heavy 0.23-mm-thick PET cover material. Platinum-type temperature sensors were attached to the MLI reflector layers identified in Figure 1 to obtain the layer temperature during cold magnet testing of the ER string. The sensor installation was performed by Bill Boroski's technical support group at FNAL. In addition, the 80-K shield temperature was monitored, but the vacuum vessel temperature was not. Figure 1 shows that sensors on the 80-K shield and reflector layer 2 bracket but do not quite isolate the heat transfer through the inner heavy cover layers. This configuration is identical with respect to the outer heavy cover layers between reflector layers 32 and 34.

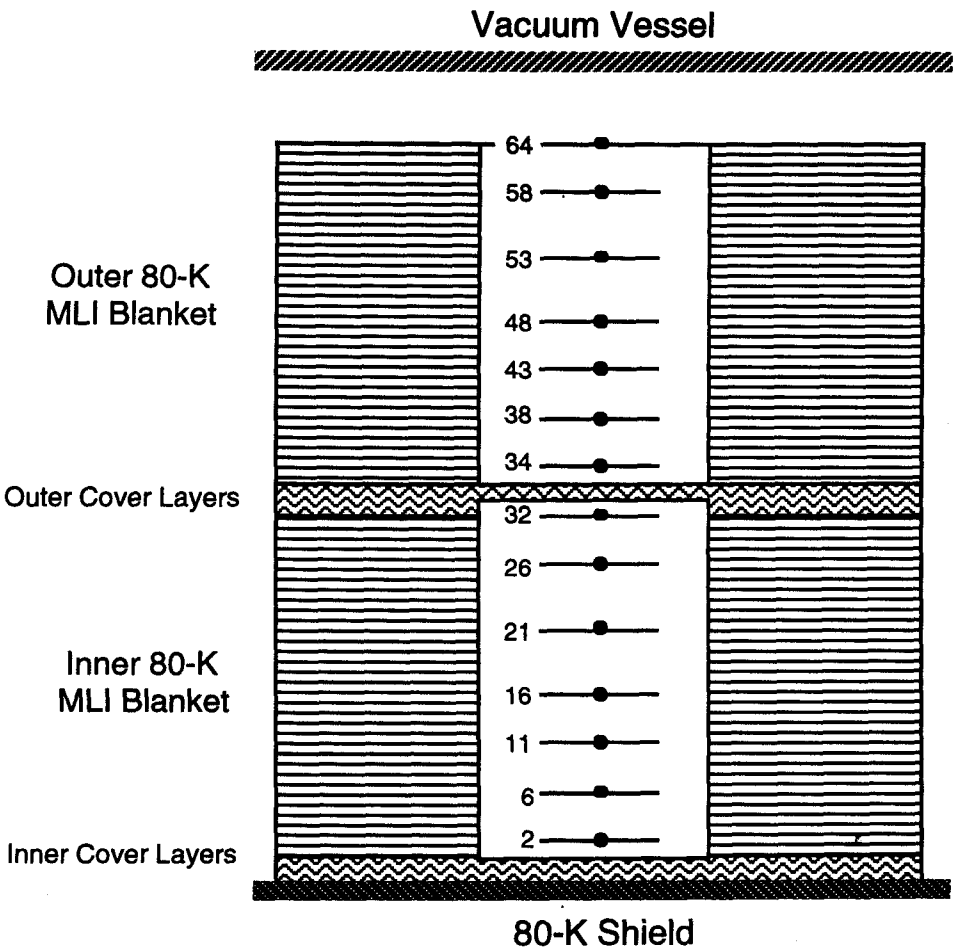

Figure 1. Thermally Instrumented 80-K MLI Blanket Assembly.

During cold testing, temperature sensor data were taken on 11 separate occasions from October 1 to November 6, 1991. In all cases the steady-state temperature gradient data were obtained by averaging measurements over a 24-hour period. The resulting data were reduced and documented by Stan Augustynowicz[1] of SSC Accelerator Cryogenics. In addition to the blanket sensor data, the vacuum pressure and composition during testing was measured by a Residual Gas Analyzer prior to, but not during, the instrumented 80-K MLI blanket testing period.

2.1 Thermal Modeling

A one-dimensional, finite-difference thermal model of the 80-K MLI blanket assembly was developed to analyze the temperature distribution data. The model, which used a standard thermal resistance capacitance network approach to describe the behavior of the system, was developed for solution using the General Dynamics Convair Thermal Analyzer (CTA) software. Zero-capacitance nodes were used to represent each reflector layer of the 80-K MLI blanket assembly and the 80-K shield. The PET spacer and cover layers were not represented with nodes but were accounted for in the thermal resistance formulation for the model. The model has unit area in the direction of heat transfer of 1 m^2. Adjacent reflector layers are connected by a triplet of parallel resistor elements that represent the components of heat transfer between the reflector layers by the modes of residual gas conduction, thermal radiation, and conduction through the spacer layers, respectively. This basic thermal network for the model is shown in Figure 2 for

a typical pair of adjacent reflector layers. This same approach is also used to model heat transfer through the cover layers between the 80-K shield and inner blanket, and the inner and outer blankets.

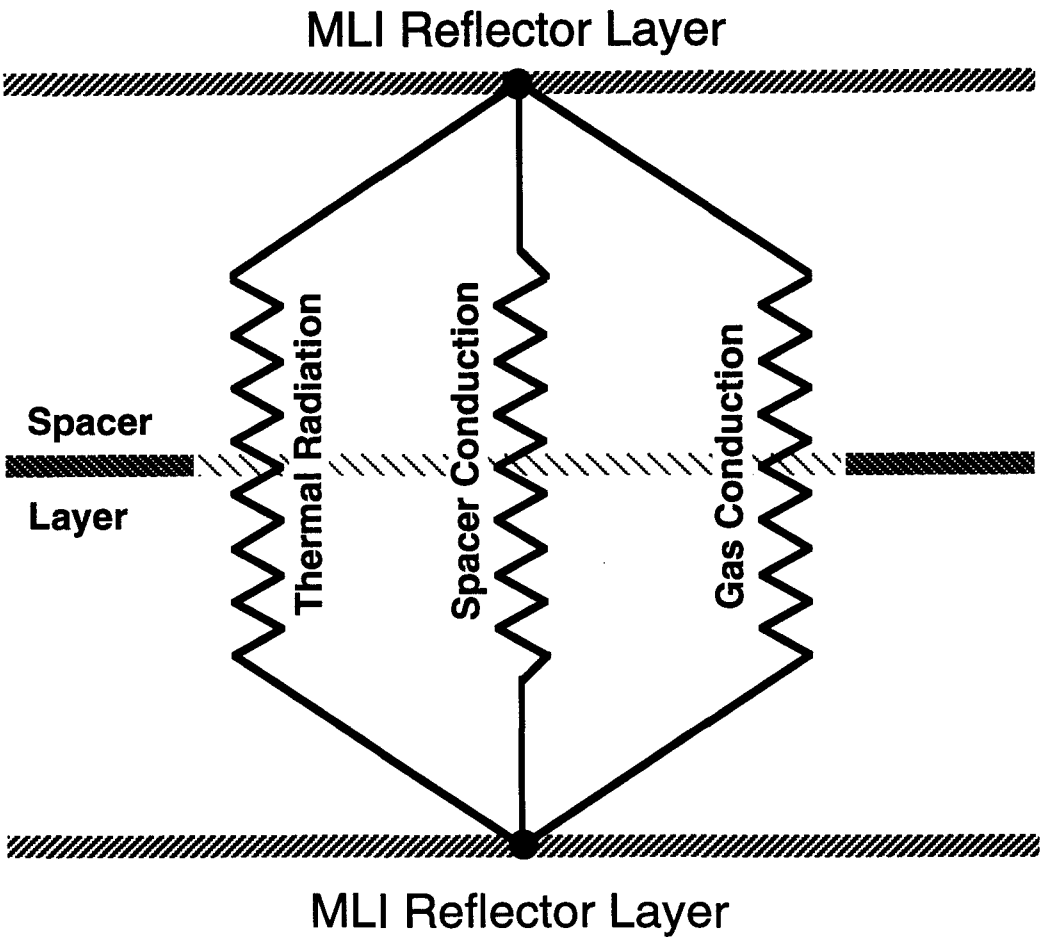

Figure 2. MLI Thermal Model.

2.1.1 Thermal Radiation Component

Heat is transferred by thermal radiation between the adjacent reflector layers and spacer layers. Within a unit area of the MLI, this process can be adequately described by a simple grey body interchange between infinite parallel planes. If the heat transfer is calculated between adjacent MLI reflector layers with an intervening spacer layer, then the heat transfer for this situation is given by:

$$Q_{\text{rad}} = \frac{\sigma A\left(T_1^4 - T_2^4\right)}{\frac{1}{\varepsilon_1} + \frac{2}{\varepsilon_s} + \frac{1}{\varepsilon_2} - 2}, \tag{1}$$

where

Q_{rad}	is the total radiant heat transfer between any two adjacent reflector layers;
A	is the total planar area of a single reflector layer;
T_1, T_2	are the temperatures of the adjacent reflector layers;
$\varepsilon_1, \varepsilon_2$	are the total hemispherical emissivities of the adjacent reflector layers; and
ε_s	is the total hemispherical emissivity of the intervening spacer layer.

Since the emissivity of the spacer layers is high (roughly 0.85) when compared to that of the reflectors (0.04), and the spacer layers are fairly transparent, the contribution of the spacer layers to the radiation heat transfer between the reflector layers can be neglected, and Eq. (1) can be simplified to:

$$Q_{rad} = \frac{\sigma A\left(T_1^4 - T_2^4\right)}{\frac{1}{\varepsilon_1} + \frac{1}{\varepsilon_2} - 1}. \tag{2}$$

Although the emissivity of the heavy cover layers is also high, the cover layers are considerably more opaque than the spacer layers. There is a pair of cover layers between the shield and inner blanket as well as a pair between the inner and outer blankets. Consequently, it was determined that in order to obtain a balance for the heat transfer between the shield/inner blanket and inner/outer blanket reflector layers separated by the heavy cover layers, the contribution of the cover layers could not be neglected. The heat transfer for this situation is given by:

$$Q_{rad} = \frac{\sigma A\left(T_1^4 - T_2^4\right)}{\frac{1}{\varepsilon_1} + \frac{4}{\varepsilon_c} + \frac{1}{\varepsilon_2} - 3}, \tag{3}$$

where ε_c is the total hemispherical emissivity of the cover layer.

The MLI total hemispherical emissivity used in this analysis varies linearly from 0.0429 at 300 K to 0.0390 at 80 K and is based on a room-temperature reflectivity measurement of DAM. The total hemispherical emissivity of the polished aluminum shield is 0.0234 at 80 K.[2]

2.1.2 Gas Conduction Component

Heat is transferred by conduction through the rarified gas existing in the evacuated space between the adjacent reflector and spacer layers. At vacuum pressures below 1E-3 torr, the gas in the vacuum space no longer behaves as a continuum substance, and the free molecular flow regime is entered. Heat is transferred by individual gas molecules between adjacent layers. This process is described by an equation given by Corruccini[3] for residual gas conduction between parallel plates. This equation is incorporated into the CTA solver program and is given by:

$$Q_{rad} = \frac{\gamma + 1}{\gamma - 1} \bullet \frac{ZPA_1(T_1 - T_2)}{\frac{1}{\alpha_1} + \frac{A_1}{A_2} \bullet \left(\frac{1}{\alpha_2} - 1\right)}, \tag{4}$$

where $Z = \sqrt{\frac{Rg_c}{8\pi MT}}$ and $T = \frac{(T_1 + T_2)}{2}$,

Q_{rad} is the total gas conduction heat transfer between any two adjacent reflector layers;
A_1, A_2 are the areas of the adjacent reflector layers;
T_1, T_2 are the temperatures of the adjacent reflector layers;
α_1, α_2 are the accommodation coefficients of the gas at the adjacent reflector layers;
P is the gas pressure in the vacuum space at the average temperature;
γ is the ratio of specific heats of the gas at the average temperature;
R is the universal gas constant;
M is the gas molecular weight; and
g_c = 32.174 lbm•ft/lbf•s^2.

The version of Eq. (4) incorporated into CTA is actually an approximation for the case where $A_1 = A_2$ and $\alpha_1 = \alpha_2$. This approximation, Eq. 5, is quite valid for the modeling of the gas conduction between adjacent reflector layers:

$$Q_{rad} = \frac{\gamma + 1}{\gamma - 1} \bullet \frac{ZPA_1(T_1 - T_2)}{\frac{2}{\alpha} + 1}. \tag{5}$$

A recent study[4] of the effects of gas modeling on the heat transfer in the magnet cryostat showed that gas conduction in the magnet thermal models should be based on a multi-species gas mixture based on empirical vacuum data. Measurements of cryostat vacuum pressure and composition performed at the FNAL ER string test with a residual gas analyzer (RGA) showed that the gas species dominant by far between 300 K and 120 K is water vapor, and below 120 K is nitrogen. Total gas pressure at the gauge was 1.5E–8 torr. However, it was also determined that a one-gas model between 300 K and 80 K was quite sufficient to describe the gas conduction component with either nitrogen or water vapor. This occurs because gas conduction is responsible for only an insignificant fraction of the total heat transfer through the 80-K MLI blanket assembly, which is dominated by thermal radiation and conduction through the spacer and reflector materials. Since the results of Reference 4 were not available during this analysis, the gas conduction component was modeled using nitrogen at the collider design vacuum pressure of 1E-6 torr. The effect of the porous spacer layers on gas conduction between the adjacent layers was ignored. Subsequent analysis of the heat transfer components showed that gas conduction represents only 0.1% of the total heat transfer in the 80-K MLI blanket assembly.

2.1.3 Spacer Conduction Component

Heat is transferred by conduction through the PET spacer or cover layers between the adjacent DAM reflector layers. This cannot be described by a simple conduction process through the spacer layer, because the irregular geometry of the spacer and reflector layers in MLI creates imperfect contact at discrete, random locations over the area normal to the direction of heat transfer. Thus heat is transferred through the spacer layers through contact resistances between the reflector and spacer materials and through normal and lateral conduction in the fibrous, anisotropic, PET material. Heat leak measurements of 80-K DAM/PET MLI blankets conducted at FNAL by Boroski have been used to empirically derive effective conductivity data for the PET spacer material. The effective conductivity values account for the effects of the various heat transfer mechanisms described above; they are germane to the specific blanket configuration tested, which was used in the ER string test instrumented blanket. The PET spacer layer effective conductivity, which has been derived from the 80-K MLI blanket component testing, is 4.171E–5 W/m•K @ 300 K, decreasing linearly to 3.602E–5 W/m•K @80 K. The spacer conduction heat transfer can then be given by:

$$Q_{sp} = \frac{k_{eff} A (T_1 - T_2)}{\Delta x}, \tag{6}$$

where

Q_{sp}	is the conduction heat transfer between any two adjacent reflector layers;
A	is the total planar area of a single reflector layer;
T_1, T_2	are the temperatures of the adjacent reflector layers;
k_{eff}	is the empirically derived PET spacer material effective conductivity; and
Δx	is the spacing between any two adjacent reflector layers.

This relation is also used for conduction through the heavy cover layers between the shield and inner blanket and inner and outer blankets. However, the effective conductivity for these cover layers was derived from the instrumented blanket temperature gradient data as described in the following section. The spacing between the reflector layers used was 0.277 mm, based on a stack height of 8.86 mm for the nominal 32-layer DAM/PET 80-K MLI blanket.

2.2 Analysis Cases

The 11 sets of steady-state temperature gradient data were analyzed using the following approach. For each set of data, three steady-state simulations were performed.

Case 1: Imposed Temperature Gradient

The model temperatures at layer locations corresponding to the sensored layers shown in Figure 1 were fixed at the measured temperatures from those locations. The remaining reflector layer temperatures were allowed to be computed by the solver program. This analysis would yield a heat flux between fixed sensor layers. If theory and the empirical spacer-effective conductivities were perfect, the resulting set of heat flux values would all be equal, since the steady-state heat transfer through the 80-K MLI blanket assembly must be constant. Consequently, these heat transfer values will be averaged to obtain the predicted heat flux through the 80-K MLI blanket assembly.

Case 2: Fixed Hot/Cold Sink Temperatures

The model temperatures at only the outermost layer of the outer blanket and the 80-K shield were fixed at the measured temperatures from those locations. This analysis is used to obtain a predicted temperature gradient through the 80-K MLI blanket assembly for comparison to the measured values. It also yields a single predicted heat flux value for comparison with the average values predicted in Case 1.

Case 3: Imposed Heat Flux

The model temperature at only the 80-K shield was fixed at the measured temperature, and the average heat flux obtained from Case 1 was imposed on the outermost layer of the outer blanket. This analysis is also used to obtain a predicted temperature gradient through the 80-K MLI blanket assembly for comparison to the measured values. The predicted gradient should closely match that obtained in Case 3.

Before each analysis case was performed for each test data set, Case 1 was analyzed for the first data set of 10/1/91 in order to determine the thermal behavior of the heavy PET cover layers. The model was initially simulated using the effective conductivity of the single spacer layers for the heavy cover layers. The predicted heat flux between the sensor locations bracketing each of the two heavy cover layer pairs (80-K shield and DAM layer 2, and DAM layers 32 and 34, respectively) was compared to the predicted heat fluxes between sensor locations immediately above those (DAM layers 2 and 6, and layers 32 and 34, respectively).

The effective conductivities and emissivities of the heavy cover layers were then independently adjusted until the heat flux through the heavy cover layers matched those predicted through adjacent MLI spacer layers to determine the behavior of the cover layers empirically. The remaining data sets were then analyzed with the effective cover layer properties derived from Case 1 of the analysis set of 10/1/91.

3.0 RESULTS

3.1 Heavy Cover Layer Effective Properties

The effective conductivity of the heavy cover layer pair between the shield and inner 80-K MLI blanket was found to be a factor of 2.1 lower than that of the spacer layers. The effective conductivity of the heavy cover layer pair between the inner and outer 80-K MLI blankets was found to be a factor of 7 lower than that of the spacer layers. For either pair of cover layers, an effective emissivity of 0.05 was required in conjunction with the conductivity adjustment to achieve a match in heat fluxes with adjacent spacer layers, and to predict a temperature gradient that agreed with the sensor data.

Since the pure conductivity of the PET material decreases with decreasing temperature, it appears contradictory that the adjustment factor for the inner cover layer pair is less than that for the outer pair. However, since the effective conductivity accounts for contact resistance effects, a plausible mechanism explains this discrepancy. The contact between the inner cover layer pair and the smooth, hard shield surface and innermost DAM reflector layer is almost certainly more intimate than the contact between the outer cover layer pair and the adjacent DAM reflector layers, since it is intentional in the design of the MLI to minimize contact between the DAM and PET layers in order to maximize resistance. Thus the inner cover layer pair could easily possess an effective conductivity higher than the outer cover layer pair due to the increased contact area and pressure between the cover layers of the inner pair versus the outer pair.

The lower effective conductivity of the heavy cover layer pair compared to the single spacer is a result of the increased conductive path length and number of layer-to-layer contact interfaces due to the presence of the two PET layers between the reflector layers. The discrepancy in the effective emissivity of the cover layers compared with the room-temperature measured value of 0.85 is probably attributable to uncertainty in the reflector layer emissivities used in the analysis. The lower-than-measured value of effective emissivity of the cover layers implies that the emissivity of the DAM reflector is lower than the 0.04 used in this analysis.

3.2 Predicted Temperature Gradients

Temperature profile predictions for the two analysis cases are shown in Figures 3 and 4. Note that average values apply to the first case, where a particular temperature gradient was imposed through the MLI blankets to replicate the ER string test profiles. The fixed values correspond to the second case, where only the temperatures of the 80-K shield and the outermost surface of the outer blanket were fixed.

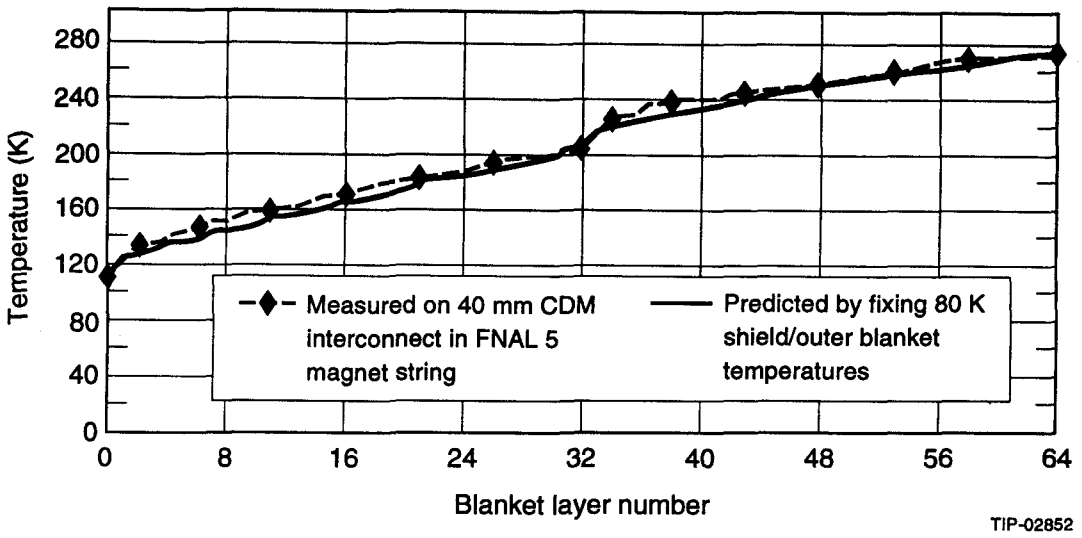

Figure 3. Comparison of Measured and Predicted Temperatures vs. Blanket Layer Number on 10/1/91.

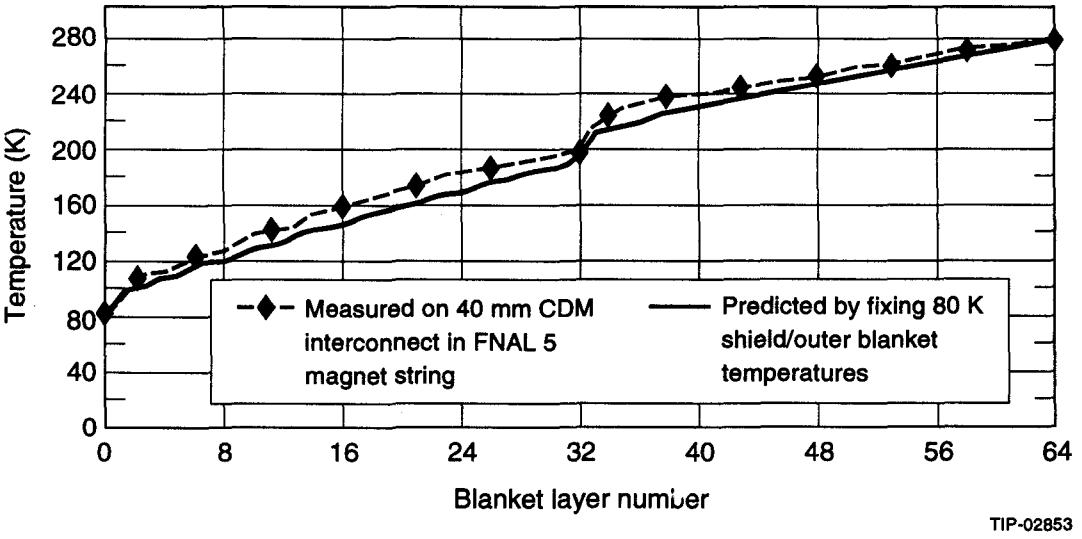

Figure 4. Comparison of Measured and Predicted Temperatures vs. Blanket Layer Number on 10/23/91.

Five of the 11 data sets were run with a nominal shield temperature of 80 K, while six were run with a nominal shield temperature of 105 K. This led to analysis cases whose difference in temperature across the MLI blankets ranged from roughly 195 K to 160 K.

The predicted temperature gradients appear much more linear through the layers than the corresponding measured temperature gradients. The measured gradients contain some curvature, although small, due to radiative heat transfer temperature dependence. This indicates that the model predicts a larger portion of heat transfer due to conduction than actually existed. Notice also that the curvature, and hence the radiative component, disappears at blanket layers above approximately N = 40. This is to be expected because temperature differences are small in this range.

3.3 Predicted 80-K Blanket Assembly Heat Flux and Gradients

The percent difference in heat flux between cases does not correlate well with the temperature difference across the MLI blanket assembly. Fixed cases were within 9% of the average cases, but the

model overpredicted the heat leak by approximately 30 mW. The ranges for the effective resistance are comparable for both case sets, but the values for the fixed cases were lower overall. This is consistent with the idea of a resistance network: as resistance increases, the heat flow will decrease for a fixed temperature difference. This implies that the cases analyzed employing fixed-end temperatures stress the conductive mode of heat transfer more than the experimental test setup. (See Table 1.)

TABLE 1. PREDICTED HEAT FLUXES AND EFFECTIVE RESISTANCES.

FNAL ER Data Set	Shield/ Outer MLI Temp. Difference K	Q_{ave} $\left(\frac{W}{m^2}\right)$	Q_{fixed} $\left(\frac{W}{m^2}\right)$	$R_{eff\text{-}ave}$ $\left(\frac{K}{\frac{W}{m^2}}\right)$	$R_{eff\text{-}fixed}$ $\left(\frac{K}{\frac{W}{m^2}}\right)$	% Difference $\left(\frac{Q_f - Q_a}{Q_a}\right)$
10/1/91*	194.78	0.453	0.473	430.07	411.54	4.50%
10/23/91	165.22	0.394	0.420	419.13	393.29	6.57%
10/24/91	167.22	0.410	0.426	407.95	393.00	3.81%
10/25/91	167.11	0.391	0.425	427.61	392.92	8.83%
10/26/91*	192.11	0.438	0.467	439.11	411.46	6.72%
10/27/91*	190.50	0.435	0.460	437.53	413.77	5.74%
11/2/91	159.22	0.365	0.397	436.58	400.86	8.91%
11/3/91	159.61	0.363	0.393	439.58	406.13	8.23%
11/4/91	168.78	0.380	0.409	443.81	412.56	7.57%
11/5/91*	185.78	0.416	0.440	446.80	422.61	5.72%
11/6/91*	186.89	0.421	0.443	444.45	421.59	5.42%

*Data set run at 80-K shield temperatures; others run at 105 K.

The results of the analysis show that the predicted total heat leak is below the heat leak budget value of 0.676 W/m^2 for static leak to the 80-K cooling system. Heat leak measurements conducted by Boroski on a single 32-layer DAM/PET MLI blanket resulted in a heat leak of 0.648 W/m^2 for a gradient of 299.7 to 79.9 K. The heat leak through two 32-layer MLI blankets between the same temperatures will not be exactly equal to half the heat leak through one blanket due to the non-linear dependence of thermal radiation on temperature. Nevertheless, as a good estimate of the effect, the measured single-blanket heat leak may be halved to compare with the results of the instrumented ER string magnet blanket. The obtained value of 0.324 W/m^2 agrees fairly well with the predicted fluxes of 0.363–0.453 W/m^2, since as observed from theory, the two-blanket heat flux must be higher.

4.0 CONCLUSIONS AND RECOMMENDATIONS

It can be concluded that these results show that the DAM/PET 80-K MLI blanket assembly is performing in the magnets comparable with design estimates and component tests, and that this performance is encouragingly below the budget leak flux.

Differences in effective conductivities of the cover and spacer layers are most likely a result of the assembly method. The MLI system relies on intermittent contact and, therefore, on high contact resistance between layers to effect the insulation scheme. This contact resistance is roughly a function of the stress imparted to the blankets during assembly. Assembly methods and procedures currently address this issue. This model reinforces the idea that process control during assembly affects blanket performance.

Residual gas conduction accounts for an insignificant portion of the total heat transfer through the 80-K MLI blanket at design vacuum.

In order to increase confidence in this model and in other thermal models, continued testing of cryogenic properties of the components that make up the MLI system is required. One particularly important set of data for this type of model is the emissivity of the DAM.

The current model predicts a heat leak whose conductive mode of heat transfer is greater than experimental results support. An effort is underway to re-evaluate the PET spacer layer effective conductivity data used in this analysis, using heat leak and temperature gradient test data for a single 32-layer 80-K MLI blanket from Boroski at FNAL. It is anticipated that refinement of this data should lower the PET effective conductivity and redress the apparent imbalance in distribution of heat transfer via the conductive and radiative modes, resulting in an improved analytical model of the MLI.

REFERENCES

1. S. Augustynowicz, internal SSC memorandum, December 5, 1991.
2. R.B. Scott, *Cryogenic Engineering*, 1963, pp. 347–348.
3. R.J. Corruccini, "Gaseous Heat Conduction at Low Pressures and Temperatures," *Vacuum*, Vol. **VII**, April 1959, pp. 19–29.
4. D.F. Franks and R.K. Pletzer, "The Effect of Vacuum Gas Pressures and Species on Internal Heat Leak in the SSCL Magnet Design," *1991 IISSC*, paper to be published.